Металлофиз. новейшие технол. / Metallofiz. Noveishie Tekhnol.
2015, т. 37, № 7, сс. 987–1000
Оттиски доступны непосредственно от издателя
Фотокопирование разрешено только
в соответствии с лицензией

Напечатано в Украине.

ЭЛЕКТРОННЫЕ СТРУКТУРА И СВОЙСТВА

PACS numbers: 61.05.Qr, 61.66.Dk, 65.40.De, 65.40.gd, 75.30.Cr, 76.80.+y, 81.05.Bx

Effect of Al Content on Magnetic Properties and Thermal Expansion of As-Cast High-Entropy Alloys $Al_xFeCoNiCuCr$

V. M. Nadutov, S. Yu. Makarenko, and Ye. O. Svystunov

G. V. Kurdyumov Institute for Metal Physics, N. A. S. of Ukraine,
36 Academician Vernadsky Blvd.,
UA-03680 Kyiv, Ukraine

The high-entropy alloys (HEA) $Al_xFeCoNiCuCr$ ($x = 1.0, 1.5, 1.8$) in cast state are investigated by means of X-ray diffraction, Mössbauer spectroscopy, magnetic and dilatometric methods. Two-phase state in the HEA and the increase of the crystal lattice parameter a of the f.c.c. and b.c.c. phases are detected. The decrease of the Curie temperature and the saturation magnetization upon deviation of Al content from equimolar composition are found out. Inhomogeneous magnetic order characterizes the studied HEA. For the studied HEA, the magnetic moment $0.2–0.4\mu_B$ and the average thermal expansion coefficient $<\alpha> = 12.4 \cdot 10^{-6}\ \mathrm{K}^{-1}$ in the temperature range of 135–545 K are determined.

Рентґеновою дифракцією, Мессбауеровою спектроскопією, магнетним і дилатометричним методами досліджено структуру та властивості високоентропійних стопів (ВЕС) $Al_xFeCoNiCuCr$ ($x = 1{,}0, 1{,}5, 1{,}8$) у литому стані. Виявлено двофазний стан ВЕС і зростання параметра кристалічної ґратниці a ОЦК- і ГЦК-фаз. Встановлено зниження температури Кюрі і намагнетованости наситу при відхилі концентрації Al від еквіатомового складу. Вивчені ВЕС характеризуються неоднорідним магнетним ладом. Для інтервалу температур 135–545 К визначено магнетний момент $0{,}2–0{,}4\mu_B$ і середнє значення температурного коефіцієнта теплового розширення $<\alpha> = 12{,}4 \cdot 10^{-6}\ \mathrm{K}^{-1}$ досліджуваних ВЕС.

Рентгеновской дифракцией, мёссбауэровской спектроскопией, магнитным и дилатометрическим методами исследованы структура и свойства высокоэнтропийных сплавов (ВЭС) $Al_xFeCoNiCuCr$ ($x = 1{,}0, 1{,}5, 1{,}8$) в литом состоянии. Выявлено двухфазное состояние ВЭС и рост параметра кристаллической решётки a ОЦК- и ГЦК-фаз. Обнаружено снижение температуры Кюри и намагниченности насыщения при отклонении содержания Al от эквиатомного состава. Изученные ВЭС характеризуются неоднородным магнитным порядком. Для интервала температур 135–545 К определён магнитный момент $0{,}2–0{,}4\mu_B$ и среднее значение темпе-

ратурного коэффициента теплового расширения $<\alpha> = 12{,}4 \cdot 10^{-6}$ К$^{-1}$ исследуемых ВЭС.

Key words: high-entropy alloys, structure, magnetic properties, thermal expansion, Mössbauer effect.

(Received March 11, 2015)

1. INTRODUCTION

Studies over the last few years of so-called high-entropy alloys (HEA) opened new opportunities to develop new structural and functional materials. By definition, HEA contain five or more different principal elements in equimolar or nearequimolar ratios. HEA may contain principal elements with the concentration of each element being between 5 and 35 at.% [1, 2]. A characteristic feature of these alloys is that they do not have the element as host.

Model conceptions of multicomponent solid solutions are applied for HEA, which are characterized by large mixing entropy as a measure of chaos and probability of single-phase state in a system minimizing a free energy $G = H - TS$. Assuming the absence of interaction between different elements, the change in the mixing entropy of n elements $\Delta S_{\max} = -R\sum_{i=1}^{n} c_i \ln c_i$ reaches a maximum for equimolar concentrations c_i and is much larger than the enthalpy change ΔH.

Contrary to theoretical assumption, it was found that HEA are crystallized in a state with two or more phases and decomposed to both dendrites and interdendrites [2–8]. It was shown in [3] that the system AlCoCrCuFeNi with the each element 0.5 or 1.0 in molar ratio exhibits simple f.c.c. and b.c.c. solid solution phases. Co, Cu, Ni elements enhance f.c.c. phase formation while Al and Cr enhance b.c.c. phase formation in the alloy systems. Along with that, the b.c.c. phase tends to form a nanospaced spinodal structure during cooling [2–4], and, in some cases, it coexists with the amorphous phase [2]. Copper tends to segregate in the interdendrite region and forms a Cu-reach f.c.c. phase [3]. The considerably inhomogeneous distribution of Cu mainly on boundaries of dendrites and other phases was reported in [5].

The lattice parameters of the f.c.c. and b.c.c. phases in the HEA $Al_xCoCrCuFeNi$ ($0 \le x \le 3$) increased with the increasing Al concentration [2, 4]. It was stated in [6] that decomposition in dendritic and interdendritic areas of equimolar HEA with the formation even six phases with different nanoscale morphology, types of structure and chemical composition occurs during the melt solidification, the following homogenization and cooling. It was shown in [7] that cooling rate

of a melt during foundry (10–20 $K \cdot s^{-1}$) or its spraying (10^6–10^7 $K \cdot s^{-1}$) have a dramatic impact on the structure and the phase composition of AlCoCrCuFeNi HEA. The homogeneous submicrocrystalline grain with b.c.c. structure was obtained just at high-rapid cooling (10^6 $K \cdot s^{-1}$) [8].

Thus, it was concluded in [9] that the modulated structure of the equimolar AlCoCrFeNiCu HEA consists of NiAl intermetallics, a (α-Fe, Cr) solid solution, some Cu enriched phase precipitates and a doubt as to the high-entropy idea to apply to multicomponent alloys was expressed.

At the same time, HEA have attracted much attention because they possess unique properties. The b.c.c. phase significantly increases hardness of the Al_xCoCrCuFeNi HEA varied within the 208–458H_V depending on Al content [3]. A solution-hardening mechanism was assumed in [2]. However, it was reported in [9] that a high-strength phase in the HEA is a NiAl intermetallic phase. High mechanical properties, strain hardening capacity and abrasive wear of the HEA Al_xCoCrCuFeNi ($0 \le x \le 3$) were revealed in [10, 11].

Due to above-mentioned properties, HEA are advanced candidates as high-strength engineering materials particularly for metallic wear-resistant, corrosion-resistant and electroconductive coatings. In this respect, the electrical and magnetic properties of HEA as well as their thermal expansion has to be investigated in all aspects of details. It was reported in [12] that as-cast, as-homogenized and as-deformed HEA Al_xCoCrFeNi exhibit high residual electrical resistivity 100–220 $\mu\Omega \cdot$cm and low temperature coefficient of resistivity 82.5 $ppm \cdot K^{-1}$ in the temperature range of 4.2–300 K.

The optimal composition of the $FeCoNi(AlSi)_x$ alloys ($0 \le x \le 0.8$) providing a balanced features like the magnetic, electrical and mechanical properties was determined in [13]. Particularly, the high saturation magnetization ($\cong$ 1.15 T) and low coercivity (1.4 A/m) were obtained, that allowed to recommend these alloys as soft-magnetic materials. Authors of [13] believe that the obtained features of HEA are caused by both high contents of the ferromagnetic metals Fe/Co/Ni and also higher atomic packing density (or atomic volume fraction) of the f.c.c. structure. It was found in [9, 14, 15, 16] that as-cast equimolar AlCoCrFeNiCu HEA displays typical ferromagnetic behaviour ($\sigma_s \cong$ 38–44 emu/g at 300 K) that on the assumption of authors is determined by spinodal decomposition in Fe–Cr-rich regions [16] or existence of paramagnetic NiAl intermetallics and magnetic solid solution (α-Fe, Cr) [9].

The data on the Curie temperature as a function of Al content in homogenized Al_xCoCrFeNi ($0 \le x \le 2$) HEA were reported in [12]. The value of T_C is relatively low and increases from 90 to 440°C with the varying concentration within the range $x = 0.25$–1.25. However, T_C of this

alloy system at $x = 2$ is uncertain quantity; particularly, it equals 375°C in [12] and 157°C in [14].

The data on thermal expansion coefficient (TEC) α of HEA are absent in literature up to now, although such a feature is important for constructions, in which HEA are joined with another materials, for example, as coatings on metal surfaces. Thermal expansion of annealed $Al_xCoCrFeNi$ ($0 \le x \le 2$) HEA was studied only at high temperatures (423–1073 K [17]). For example, for HEA with $x = 1$, two minima on temperature dependence of α were detected at 844.1 K and 920 K, the first of which is attributed to the Curie temperature and the second one is identified as σ-phase precipitation that has a NiCoCr structure. The TEC decreased with the increasing aluminium content x. However, it could be noted that the derived TEC of the HEA does not characterize their thermal expansion nearby and below the room temperature at which the diffusion processes are slowed down. In addition, the Curie temperature obtained in [17] is inconsistent with the much lower values of $T_C = 200–440$ K reported in [12].

Thus, the aim of this work was to study the magnetic properties and thermal expansion of the as-cast $Al_xFeCoNiCuCr$ HEA at the temperatures below 650 K depending on deviation of Al content from equimolar composition ($x = 1$, 1.5, and 1.8). The distribution of the hyperfine magnetic fields at iron nuclei in one of the HEA ($x = 1.5$) was analysed on the basis of the Mössbauer data.

2. MATERIAL AND METHODS

The $Al_xFeCoNiCuCr$ alloy ingots with the Al content of $x = 1$, 1.5, and 1.8 were prepared by a vacuum ark melting of mixture of elements Al, Fe, Co, Ni, Cu, Cr with the purities of better than 99.9 wt.%. The chemical composition of the alloys was determined by X-ray fluores-

TABLE 1. Chemical composition of the $Al_xFeCoNiCuCr$ alloys.

Sample	x	wt.%					
		Al	Fe	Co	Ni	Cu	Cr
A_1	1.0	8.8	18.1	18.3	18.9	19.7	16.0
A_2	1.5	12.2	17.4	17.3	18.6	19.4	14.9
A_3	1.8	14.9	16.8	17.1	17.7	18.7	14.7
		at.%					
A_1	1.0	17.2	17.1	16.3	16.9	16.3	16.2
A_2	1.5	23.0	15.9	14.9	16.1	15.5	14.6
A_3	1.8	27.3	14.9	14.4	14.8	14.6	14.0

cence analysis (see Table 1).

The rectangular specimens of 10–15 mm in length were machined for X-ray diffraction analysis and measurements of properties. Foils of 20–30 μm in thick for Mössbauer measurements were performed by mechanical polishing of plates and following etching in acid.

The structure and the phase composition of the alloys were studied by means of X-ray diffraction analysis at room temperature using 'DRON-3M' diffractometer and CoK_α-radiation. Before measurements, a layer of 0.2–0.25 μm in thickness was etched from a sample surface in order to eliminate a probable hardening after machining.

The field dependence magnetization of the HEA was measured by means of ballistic magnetometer at 293 K in the magnetic field of 0–800 kA·m^{-1}, and using these curves the saturation magnetization was estimated. The alternating current (AC) magnetic susceptibility was measured in a temperature range of 80–650 K by means of induction method based on the compensated transformer using weak magnetic field of a 400 A·m^{-1} in magnitude and 1 kHz in frequency.

The dilatometric measurements were carried out in the induction quartz dilatometer within the temperature range 135–530 K. The initial longitudinal sample size l = 12–13 mm was measured with an accuracy of ±0.005 mm. The calculations of TEC were performed using software, which provides smoothing of the experimental curves and the accuracy of $\pm 0.3 \cdot 10^{-6}$ K^{-1}.

The Mössbauer measurements were performed at room temperature using a MS 1101E spectrometer. The γ-quantum source was the ^{57}Co isotope of 5 μCi in radioactivity. Velocity calibration and the isomer shifts were estimated with respect to α-Fe foil. The accuracy of the velocity measurements was 0.016 mm/s in the range of ±8 mm/s. The Mössbauer spectrum was treated by Window method.

3. RESULTS AND DISCUSSION

3.1. X-Ray Diffraction Analysis

In order to certify samples and compare with the known data, the X-ray diffraction analysis was carried out. The measurements revealed the f.c.c. and b.c.c. phases in the cast Al$_x$FeCoNiCuCr HEA (Fig. 1) that is in accordance with the data reported previously in [1–4]. The equimolar HEA A_1 consists of b.c.c. and two f.c.c.$_1$ and f.c.c.$_2$ phases, although the HEA A_2 (x = 1.5) and A_3 (x = 1.8) contain just b.c.c. and one f.c.c.$_1$ phases. The f.c.c.$_2$ phase in the A_2 and A_3 HEA was not detected. The lattice parameters of the phases in the equimolar HEA A_1 are $a_{\text{b.c.c.}}$ = 0.2871 nm, $a_{\text{f.c.c.}_1}$ = 0.3624 nm, and $a_{\text{f.c.c.}_2}$ = 0.3592 nm. The parameters $a_{\text{b.c.c.}}$ and $a_{\text{f.c.c.}_1}$ increased with the increasing Al content in the HEA A_2 and A_3 (see Table 2). For example, in the case of A_3 sample,

the increment for $a_{\text{b.c.c.}}$ is 0.38% and for $a_{\text{f.c.c.}_1}$ it is 0.66%. This means that Al was dissolved in both phases. The obtained results are consistent with the concentration dependence of the lattice parameter of the b.c.c. and f.c.c. phases in the Al_xFeCoNiCuCr HEA reported in [2, 4].

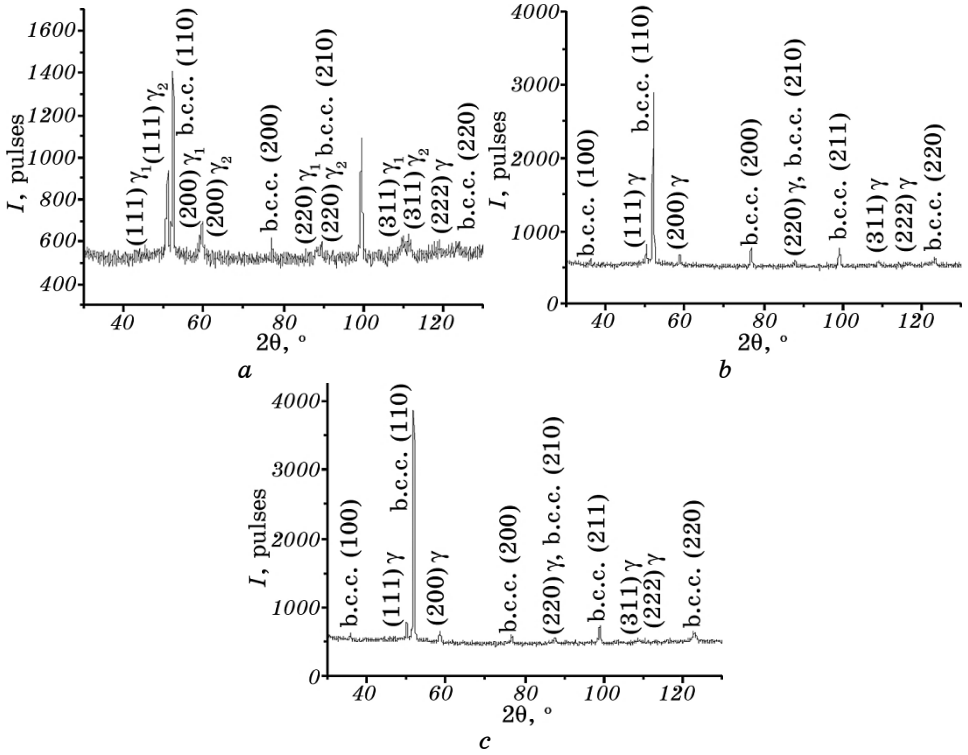

Fig. 1. The diffraction patterns of the Al_xFeCoNiCuCr HEA: $x = 1$ (A_1) (*a*), $x = 1.5$ (A_2) (*b*), $x = 1.8$ (A_3) (*c*).

TABLE 2. The lattice parameters of phases in the Al_xFeCoNiCuCr HEA.

Sample	x	a, nm					
		Cast state			After heating to 650 K during measurements of $\chi(T)$		
		b.c.c.	f.c.c.$_1$	f.c.c.$_2$	b.c.c.	f.c.c.$_1$	f.c.c.$_2$
A_1	1.0	0.2871	0.3624	0.3592	0.2871	0.3627	0.3600
A_2	1.5	0.2877	0.3643	–	0.2880	0.3639	–
A_3	1.8	0.2882	0.3648	–	0.2885	0.3643	–

3.2. Magnetic Properties

Two-phase state of the HEA is reflected in behaviour of the magnetic properties. The Curie temperature of the HEA was estimated upon the temperature dependence of the magnetic susceptibility χ (Fig. 2). Note that the magnetic transition in all samples occurs in broadened temperature range. For the equimolar alloy A_1, the Curie temperature $T_{C1} = 352$ K (Fig. 2, *a*). This is close to that obtained upon magnetization curve for the as-cast HEA of similar composition [15] and lies between temperatures 200 K and 440 K obtained in [12] for the HEA $Al_xCoCrFeNi$ with $x = 0.75$ and 1.25, respectively. However, this magnetic transition was not reported in work [14], where saturation magnetization of as-cast equimolar HEA *vs* temperature was analysed.

The Curie temperature T_{C1} decreases with the deviation from equimolar composition: $T_{C1} = 282$ K at the Al content $x = 1.8$ (Fig. 2, *c*, Fig. 3). This correlates with the reduction of the saturation magnetisation curve (Fig. 3). It is obvious since the crystal lattice constant of the

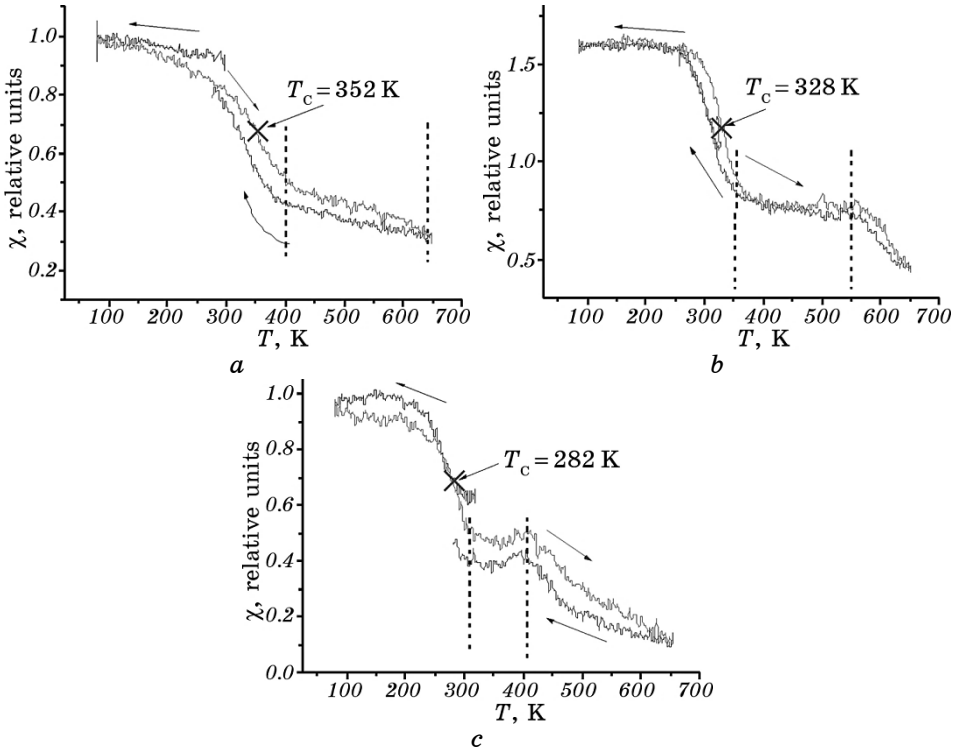

Fig. 2. The temperature dependence of the magnetic susceptibility χ of the HEA $Al_xFeCoNiCuCr$: $x = 1$ (A_1) (*a*), $x = 1.5$ (A_2) (*b*), $x = 1.8$ (A_3) (*c*). The temperature interval with the flattening of $\chi(T)$ is denoted by vertical dash lines.

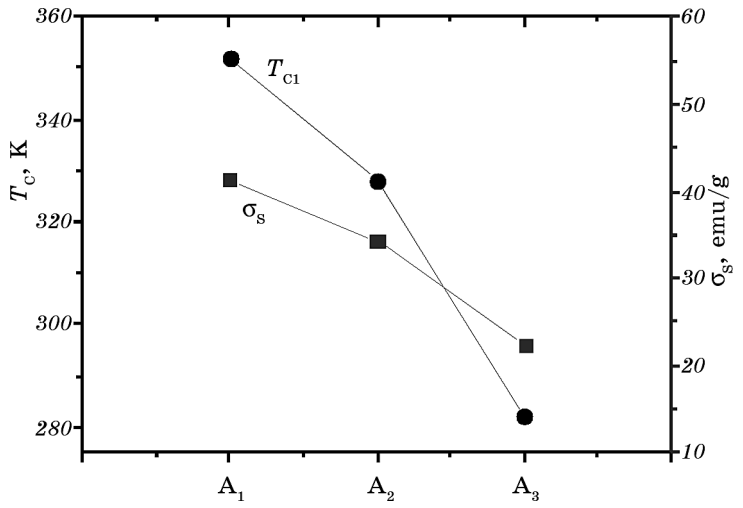

Fig. 3. The Curie temperature and the saturation magnetisation of the HEA Al_xFeCoNiCuCr *vs* Al content.

alloy growths with the addition of Al content (Table 2) that results in weakening exchange interaction.

The slope of the heating curve $\chi(T)$ for the equimolar HEA A_1 above 400 K slightly decreases (Fig. 2, *a*). The complete flattening of the $\chi(T)$ curve arises for the A_2 alloy ($x = 1.5$) within the temperature range of 350–550 K (Fig. 2, *b*). At the same time, the curve flattening for the HEA A_3 ($x = 1.8$) starts at 300 K and this dependence $\chi(T)$ even slightly increases at 400 K (Fig. 2, *c*). The flattening temperature interval is gradually narrowed. At the following elevating temperature above 550 K and 400 K for the alloys A_2 and A_3, respectively, a further dramatic reduction of the magnetic susceptibility occurs (Fig. 2, *b*, *c*).

Since changes in the $\chi(T)$ curves are observed at relatively low temperatures, at which structural phase transformations do not occur [4, 14, 16], one can assume that at least two magnetic transitions in the studied HEA are realized. The magnetic nature of the observed changes against temperature is supported by almost reversible behaviour of the cooling curves (Fig. 2). Although the Curie point T_{C1} of the alloys was determined relatively simple, it was difficult to estimate the second temperature T_{C2} using available $\chi(T)$ data. At the same time, two magnetic transitions comply with the X-ray diffraction data regarding two phase states (Fig. 1). In order to determine distinctly these magnetic transitions, the temperature dependence of the saturation magnetization σ_s of the as-cast equimolar HEA (A_1) was measured in magnetic field of 800 kA·m^{-1} (Fig. 4). Two magnetic transitions at $T_{C1} = 440$ K and $T_{C2} = 925$ K were detected. In this experiment, the Curie temperature T_{C1} is higher than that derived from magnetic suscep-

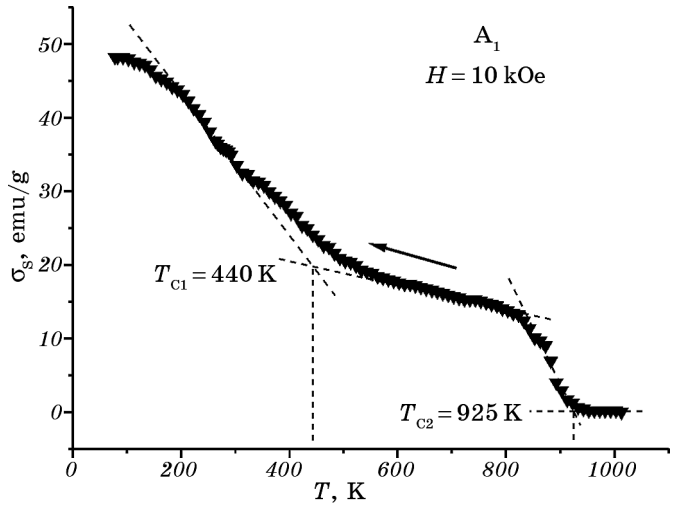

Fig. 4. The saturation magnetization of the as-cast equimolar Al_xFeCoNiCuCr HEA (A_1 $x = 1$) *vs* cooling temperature. Vertical dash lines denote the Curie temperatures.

tibility curve (Fig. 2) that results from the effect of relatively large magnetic field.

Based on the investigations in details by TEM of the equimolar AlFeCoNiCuCr HEA, it was shown [7, 9] that as-cast alloy is not uniformly distributed solid solution and comprised several b.c.c. and f.c.c. phases, which differ from each other by both composition and type of atomic ordering. It is unlikely that a plate-like Cu-rich (of $B2$ structure) and rhombohedron-shaped Cu-rich precipitates (of $L1_2$ structure, f.c.c.$_1$ and f.c.c.$_2$) in dendrite and interdendrite regions containing small amounts of magnetics [7] could considerably contribute to the magnetic behaviour of the HEA. Along with those, the Al–Ni-rich plates of $B2$ structure and Cr–Fe-rich interplates of b.c.c. structure [7, 16] may show ferromagnetism and different Curie points.

As reported in [9], the NiAl intermetallic is weak magnetic phase in HEA. Moreover, Ni–Al alloy shows ferromagnetism, and the concentration of 25% Al provides the Curie temperature 343 K [18], which is close to the obtained $T_{C1} = 352$ K for the as-cast equimolar HEA (Fig. 2). Weak discrepancy between these values was expected because the elements Co, Fe, Cr are not uniformly distributed in the studied HEA, particularly, in the Al–Ni-rich regions [7, 16]. Due to that, the magnetic transition nearby T_{C1} is rather broad and smeared (Fig. 2, *a*, Fig. 4).

Along with that, the second Curie temperature T_{C2} of the as-cast HEA alloy most probably resulted from existence of Cr–Fe-rich regions. In fact, as assumed in [9], the (α-Fe, Cr) solid solution is magnetic phase in as-cast HEA. In addition, it was reported in [16] that the

ferromagnetic behaviour of the HEA results from spinodal decomposition of Fe and Cr in Fe–Cr-rich regions on a scale of few nanometres. This complies with the data [19] that two-phase microstructure (Fe-rich α_1- and Cr-rich α_2-phases) on the nanometre scale formed during spinodal decomposition determines magnetic properties of ternary Fe–Co–Cr alloys.

A weak irreversibility of the cooling curves $\chi(T)$ as compared to the heating ones is observed (Fig. 2). Since samples were heated to 650 K during measurements that was lower than the miscibility gap of spinodal decomposition (871–913 K) [4, 16] and the phase transformation [14], this irreversibility results from diffusion processes and atomic redistribution in a solid solution at heating influencing on interatomic distance and, consequently, on exchange interaction. In fact, the lattice constants a of the f.c.c.$_1$ and f.c.c.$_2$ phases in equimolar HEA ($x = 1$) increased after the magnetic susceptibility measurements by approximately 0.1% and 0.2%, respectively, and the difference between them gradually decreases. The lattice constants of the phases in the A_2 ($x = 1.5$) and A_3 ($x = 1.8$) alloys are also changed after the measurements of the $\chi(T)$ dependence (see Table 2).

The saturation magnetization of the Al_xFeCoNiCuCr HEA was taken from the dependences of the magnetization at $T = 293$ K against magnetic field (Fig. 5). It is noteworthy that the considerably low saturation magnetization $\sigma_s = 41.3$ emu/g of the as-cast equimolar HEA A_1 ($x = 1$) is compared to pure metals (Fe, Ni, Co) [20]. Moreover, the σ_s value de-

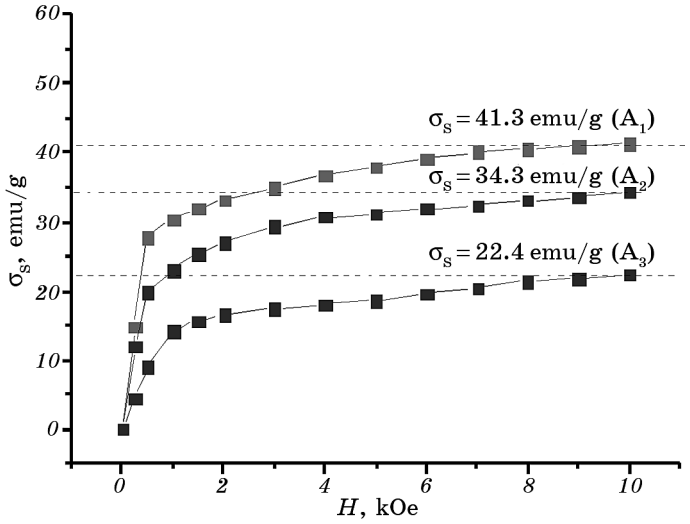

Fig. 5. Magnetization curves of the Al_xFeCoNiCuCr HEA ($x = 1$, 1.5, 1.8) at room temperature. The extrapolated dashed lines denote saturation magnetization σ_s.

clines as Al content increases: $\sigma_s = 34.3$ emu/g for $x = 1.5$ and $\sigma_s = 22.4$ emu/g for $x = 1.8$ (Figs. 3, 5). The obtained result complies with the change of the Curie temperatures (Fig. 3). Low σ_s of as-cast HEA was also reported in [9, 14–16] and its reduction in annealed at 1100°C HEA with the Al content in the range $1.25 \le x \le 2.0$ was revealed in [12]. Cause of the reducing ferromagnetism of the HEA is the weakening of the exchange interspin interaction due to increasing of the interatomic distance (Table 2) and screening by diamagnetic Al and Cu.

Assuming the additive contribution of the magnetic moments of each metals, Fe ($\mu = 2.2\mu_B$), Ni ($\mu = 0.6\mu_B$), Co ($\mu = 1.7\mu_B$), in ferromagnetism [20] and taking into account their total content $<c_{Fe,Ni,Co}> \cong \cong 50\%$, an average magnetic moment of the HEA $<\mu> = 0.75\mu_B$ was expected. However, taking into account the ratio $<\sigma_s> \cong 100<\mu_{exp}>$ [20] and the obtained data for σ_s (Fig. 5), the experimental value is $<\mu_{exp}> = 0.2–0.4\mu_B$. The obtained $<\mu_{exp}>$ complies with the low value of the most probable hyperfine magnetic field $H = 13$ T derived in Mössbauer experiment for the $Al_{1.5}FeCoNiCuCr$ alloy (Fig. 6). Taking into account the linear relationship between the hyperfine magnetic field and the magnetization, $H[\text{Oe}] = A<M> + B\mu_B$, and the magnitude of coefficient $B = 120$ that denotes a field at iron nuclei induced by one Bohr magneton [21], the coefficient $A = 13.2$ was estimated. In this case, $<M> = \rho\sigma_s$, where ρ is the mass density 7.035 g/cm^3 for the $Al_{1.5}FeCoNiCuCr$ HEA.

Wide distribution of the hyperfine magnetic fields 0–40 T (Fig. 6, *b*) points to existence of different atomic configurations in b.c.c. and f.c.c. phases of the HEA including nearest surroundings of Fe atoms by magnetic and nonmagnetic elements. In accordance with the Slater–Pauling diagram [21], the most probable atomic bonds are varied from the Fe–Co with the maximum $<\mu>$ and H to the Ni–Cu with the nearly zero values of these quantities. This complies with the idea [16] that

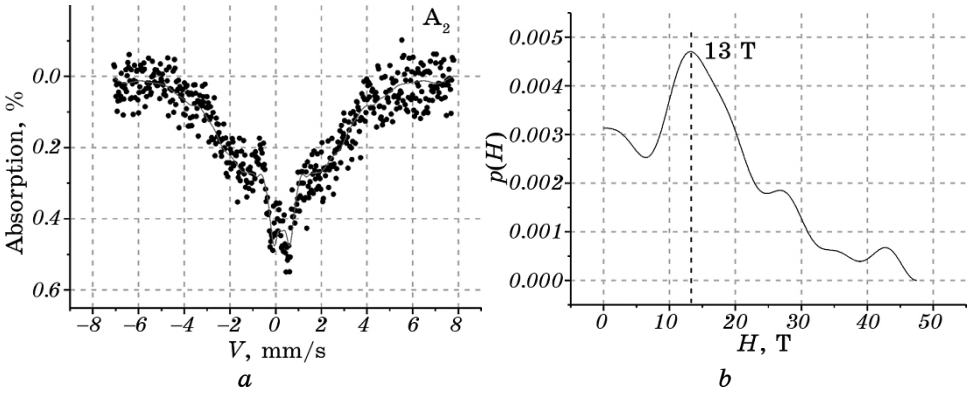

Fig. 6. ^{57}Fe Mössbauer spectrum of the HEA $Al_xFeCoNiCuCr$ ($x = 1.5$) (*a*) and distribution of the hyperfine magnetic fields on Fe nuclei (*b*).

there are regions in HEA decompose into ferromagnetic Fe–Co-rich and antiferromagnetic Cr-rich domains.

3.3. Thermal Expansion

The temperature dependences of thermal expansion coefficient (TEC)

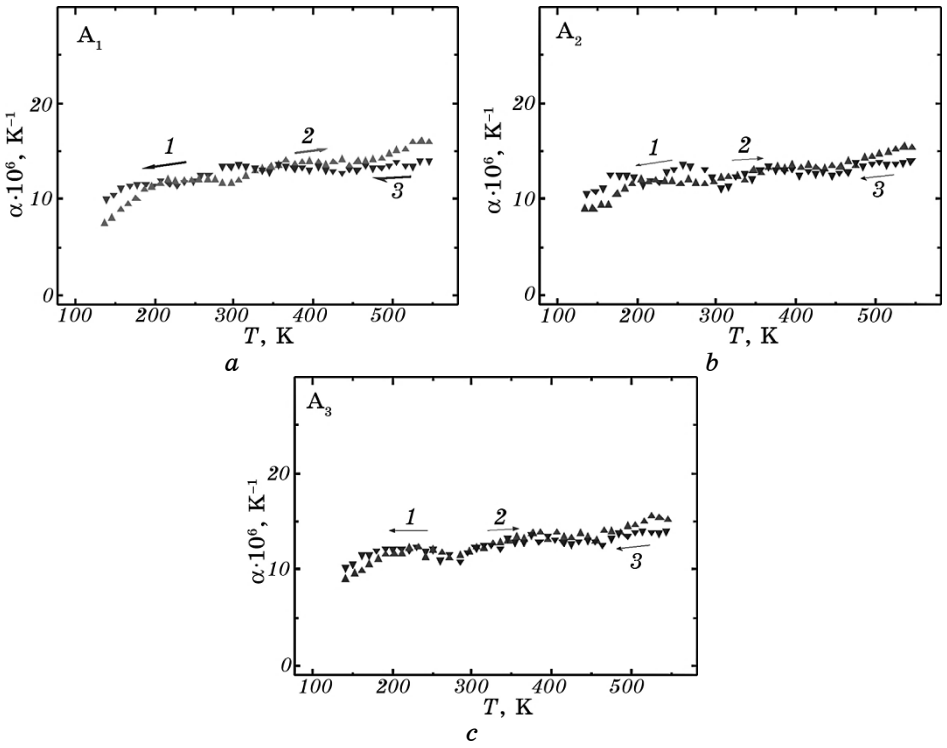

Fig. 7. The TEC of the $Al_xFeCoNiCuCr$ HEA: $x = 1$ (A_1) (*a*), $x = 1.5$ (A_2) (*b*), $x = 1.8$ (A_3) (*c*).

TABLE 3. The thermal expansion coefficient of the $Al_xFeCoNiCuCr$ HEA.

Sample	x	α, K^{-1}		
		200–500 K		135–545 K
		α_{min}	α_{max}	$<\alpha>$
A_1	1.0	$11.4 \cdot 10^{-6}$	$14.8 \cdot 10^{-6}$	$12{,}3 \cdot 10^{-6}$
A_2	1.5	$11.8 \cdot 10^{-6}$	$14.5 \cdot 10^{-6}$	$12{,}4 \cdot 10^{-6}$
A_3	1.8	$11.5 \cdot 10^{-6}$	$14.5 \cdot 10^{-6}$	$12{,}4 \cdot 10^{-6}$

of the investigated HEA in temperature range (135–545) K are presented in Fig. 7. The minimal and maximal values of TEC in the temperature range 200–500 K and its average values within the range 135–545 K are summarized in Table 3. The close values of TEC for all studied HEA indicate similar their thermal expansion behaviour in the considered temperature range. This is not consistent with the data reported in [17] that α decreases with the increasing Al content. The disagreement is explained by special thermal treatment of HEA before measurements and higher temperatures range for measurements in [17] as compared to those in our case.

It should be noted that the TEC of all investigated HEA at 300 K has approximately the same value $12.0 \cdot 10^{-6}$ K^{-1} that very differs from α of pure metals Al, Cu, Cr, but close to this value for Fe, Co, Ni and the alloys on their basis, in particular ferrite steels [22, 23]. This fact means that the Al_xFeCoNiCuCr HEA can be connected with steel items or deposited as coatings on their surfaces to increase hardening and wear resistance.

4. CONCLUSION REMARKS

The broadened temperature range of the magnetic transition and wide distribution of the hyperfine magnetic fields (0–40 T) on Fe nuclei was found out that points to inhomogeneous magnetic order in the as-cast equimolar Al_xFeCoNiCuCr ($x = 1$, 1.5, 1.8) HEA resulting from their two-phase state and inhomogeneous atomic distribution in a solid solution containing Al–Ni-, Fe–Cr-, Fe–Co-, Ni–Cu-rich atomic configurations.

The Curie temperature $T_C = 352$ K and the saturation magnetization 41.3 emu/g of the as-cast equimolar HEA are much lower as compared to those for pure metals and these quantities decreased to 282 K and 22.4 emu/g, respectively with the increasing Al concentration. The estimated average magnetic moments of the as-cast Al_xFeCoNiCuCr HEA are 0.2–0.4μ_B.

An average thermal expansion coefficient of the studied HEA for the temperature range of 135–545 K is $<\alpha> = 12.4 \cdot 10^{-6}$ K^{-1}, and it is principally independent on Al content for $x = 1$, 1.5, 1.8. In a temperature range of 200–500 K, the value of α is changed within the narrow interval $11.4–14.8 \cdot 10^{-6}$ K^{-1} that close to that for ferrite steels and points to opportunity to apply the Al_xFeCoNiCuCr HEA as a materials for deposition of hardened and wear resistant coatings.

The authors expressed their gratitude to V. P. Zalutskii for X-ray measurements and to T. V. Efimova for the measurements of field dependence of the magnetization of HEA.

The work was done with the financial support of the competitive project 22/15-N of the targeted comprehensive program of fundamen-

tal research of the N. A. S. of Ukraine ‘Fundamental problems of creating new nanomaterials and nanotechnology’.

REFERENCES

1. S. Ranganathan, *Curr. Sci.*, **85**: 1404 (2003).
2. J. W. Yeh, S. K. Chen, S. J. Lin, J. Y. Gan, T. S. Chin, T. T. Shun, C. H. Tsau, and S. Y. Chang, *Adv. Eng. Mater.*, **6**: 299 (2004).
3. Ch.-Ch. Tung, J.-W. Yeh, T.-T. Shun, S.-K. Chen, Yu.-Sh. Huang, and H.-Ch. Chen, *Mater. Lett.*, **61**, Iss. 1: 1 (2007).
4. C. J. Tong, Y. L. Chen, S. K. Chen, J. W. Yeh, T. T. Shun, C. H. Tsau, S. J. Lin, and S. Y. Chang, *Metall. Mater. Trans. A*, **36**: 881 (2005).
5. V. M. Nadutov, S. Yu. Makarenko, P. Yu. Volosevych, and V. P. Zalutskii, *Metallofiz. Noveishie Tekhnol.*, **36**, No. 10: 1327 (2014).
6. M. V. Ivchenko, V. G. Pushyn, A. N. Uksusnikova, N. Wanderka, and N. I. Kourov, *Phys. Met. Metallogr.*, **114**: 561 (2013).
7. S. Singh, N. Wanderka, B. S. Murty, U. Glatzel, and J. Banhart, *Acta Mater.*, **59**: 182 (2011).
8. M. V. Ivchenko, V. G. Pushyn, and N. Wanderka, *J. Tech. Phys.*, **84**: 57 (2014).
9. Y. P. Wang, B. Sh. Li, and H. Zh. Fu, *Advan. Eng. Mater.*, **11**: 641 (2009).
10. C. J. Tong, Y. L. Chen, S. K. Chen, J. W. Yeh, T. T. Shun, C. H. Tsau, S. J. Lin, and S. Y. Chang, *Metall. Mater. Trans. A*, **36**: 1263 (2005).
11. J. M. Wu, S. J. Lin, J. W. Yeh, S. K. Chen, Y. S. Huang, and H. C. Chen, *Wear,* **261**: 513 (2006).
12. Y. F. Kao, S. K. Chen, T. J. Chen, P. C. Chu, J. W. Yeh, and S. J. Lin, *J. Alloys Compd.*, **509**: 1607 (2011).
13. Y. Zhang, T. T. Zuo, Y. Q. Cheng, and P. K. Liaw, *Sci. Rep.*, **3**: 1 (2013).
14. M. S. Lucas, L. Mauger, J. A. Munoz, Yuming Xiao, A. O. Sheets, S. L. Semiatin, J. Horwath, and Z. Turgut, *J. Appl. Phys.*, **109**: 07E307 (2011).
15. K. B. Zhang, Z. Y. Fu, J. Y. Zhang, J. Shi, W. M. Wang, H. Wang, Y. C. Wang, and Q. J. Zhang, *J. Alloys Compd.*, **502**: 295 (2010).
16. S. Singh, N. Wanderka, K. Kiefer, K. Siemensmeyer, and J. Banhart, *Ultramicroscopy*, **111**: 619 (2011).
17. H. P. Chou, Y. S. Chang, S. K. Chen, and J. W. Yeh, *Mater. Sci. Eng.*, **163**: 184 (2009).
18. A. E. Vol, *Structure and Properties of Binary Metal Systems* (Moscow: Gos. Izd. Fiz.-Mat. Liter.: 1959), vol. **1** (in Russian).
19. W. Martienssen and H. Warlimont, *Springer Handbook of Condensed Matter and Materials Data: Functional Materials* (Berlin–Heidelberg: Springer-Verlag: 2005), p. 795.
20. C. Kittel, *Introduction to Solid State Physics* (Moscow: Nauka: 1978) (Russian translation).
21. G. Wertheim, *Mössbauer Effect: Principles and Applications* (Moscow: Mir: 1966) (Russian translation).
22. L. N. Larikov and Yu. F. Yurchenko, *Structure and Properties of Metals and Alloys* (Kiev: Naukova Dumka: 1985) (in Russian).
23. S. I. Novikova, *Thermal Expansion of Solids* (Moscow: Nauka: 1974) (in Russian).